European Journal of Pharmaceutics and Biopharmaceutics 74 (2010) 442–450

Contents lists available at ScienceDirect

European Journal of Pharmaceutics and Biopharmaceutics

journal homepage: www.elsevier.com/locate/ejpb

Research paper

Efficacy of surface charge in targeting pegylated nanoparticles of sulpiride to the brain

Tapan Parikh *, Murali Mohan Bommana, Emilio Squillante III

Department of Pharmacy and Administrative Sciences, Saint Johns University, New York, United States

ARTICLE INFO

Article history:
Received 23 February 2009
Accepted in revised form 4 November 2009
Available online 24 November 2009

Keywords:
Adsorption
Albumin
Blood–brain barrier
Cationized bovine serum albumin
CNS
Drug targeting
Pegylation
Microscopy
Nanoparticles
Sulpiride
Surface charge

ABSTRACT

The objective of the study was to formulate sulpiride-loaded nanoparticles (NPs) that can improve bioretention and achieve dose reduction by passively targeting the drug near the site of action. Methoxy PEG–PLA and maleimide PEG–PLA were synthesized via ring opening polymerization of L-lactide and used to prepare pegylated nanoparticles (NPs) loaded with sulpiride by emulsification and solvent evaporation method. Thiolated cationized bovine serum albumin (CBSA) was conjugated through the maleimide function to the NPs. Rhodamine B and Alexa Fluor® 488 were used as fluorescent markers for nanoparticle uptake studies. The nanoparticles were characterized for particle size, zeta potential and drug loading. Sprague Dawley rats were administered with each of CBSA-NPs, BSA-NPs and uncoated NPs (10 mg/kg) via tail vein; plasma and urine concentrations were measured and tissue sections were observed under fluorescence microscope. Characterized particles (mean particle size 329 ± 44 nm) indicated the conjugation of cationic albumin to NPs (zeta potential shift from −39 mV to −19 mV). Fluorescence showed a high accumulation of CBSA-NPs in brain compared to that of BSA-NPs and uncoated NPs supported by plasma and urine profile. The significant results proved that CBSA-NPs could be a promising brain drug delivery for sulpiride.

1. Introduction

Colloidal carriers present a useful strategy to circumvent barriers against the entrance of drug into the central nervous system (CNS). Penetration is enhanced when such carriers are embellished with ligands, antibodies and proteins as a targeting moiety [1]. The accepted view posits a blood–brain barrier (BBB) of endothelial cells with tight junctions supported by astrocyte foot processes through which small molecules or lipophilic moieties pass easily relative to the hydrophilic moieties [1]. It is logical to expect that passive diffusion of xenobiotic into the CNS ought to be enhanced if NPs were retained longer adjacent to brain capillary walls because the higher concentration presents a diffusion gradient, thereby elevating transport rates across the endothelial cell layer. Others have posited a "membrane fluidization" effect across the endothelial cell membrane because of surfactant effect of NPs coatings [2]. Such methods modify the diffusional resistance and suffer from the ever present liability that removing the barrier to one xenobiotic does so for others. A more selective scheme capitalizes on physical size, as it is now apparent NPs permeate through the BBB by the opening of the tight junctions between the endothelial cells once a certain size threshold has been crossed [1], in which case the drug bound inside the particle is leached over a period of time, creating a controlled, sustained release rate [3,4]. A review of the literature shows that constraining production methods to excipients generally regarded as safe, and conditions that do not challenge stability profiles of most drugs leaves most particle diameters lamentably higher than this target. The above mechanisms could work in single or concert to affect the brain uptake of NPs but a truly interesting question might be: "Is it desirable to create conditions that nullify the role of the BBB to the extent that NPs are transcytosed into the brain parenchyma?" There are real advantages to a negative response to this such as less stringent demand to produce smaller less stable particles. Perhaps a safe, efficient alternative is a surface embellishment of cationized proteins attached to NPs to promote attachment to the negative-charged luminal side of the endothelial cells [5]. Biodegradable poly-(lactide-co-glycolide) (PLGA) and poly-(lactide) (PLA) polymers enjoy FDA acceptance and are biocompatible. "Pegylation" (i.e., addition of PEG chains) to these biodegradable polymer increases the persistence of NP's in the plasma, presumably due to decreased uptake and elimination by the reticuloendothelial cells. CBSA-NPs labeled with dyes such as 6-coumarin shows positive re-

* Corresponding author. Address: Department of Pharmacy and Administrative Sciences, College of Pharmacy, Saint Johns University, 8000 Utopia Parkway, Queens, New York 11439, United States. Tel.: +1 917 385 4178; fax: +1 816 841 4634.
E-mail address: tapangp@gmail.com (T. Parikh).

0939-6411/$ - see front matter © 2009 Elsevier B.V. All rights reserved.
doi:10.1016/j.ejpb.2009.11.001

sults for a better CNS delivery system [5]. In vitro toxicity studies showed that CBSA-NPs are better than the uncoated NPs because of the targeting moiety [6]. Sulpiride (e.g. Dogmatil Forte® 200 mg oral tablets) [7] being practically insoluble in water results in low oral absorption with 30% bioavailability. Additionally, as described by Wiesel et al. [8], 70–90% of dose is excreted unchanged in urine with the half-life of 6–8 h making it an ideal candidate for our study. Considering the above given information, we chose to investigate cationized sulpiride-loaded nanoparticles when compared to the uncationized delivery system as a targeted delivery form in Sprague Dawley rats.

The principal objective of the study was to assess the efficacy of positively charged particles to achieve selective accumulation of sulpiride near the site of action by improved bioretention and hence dose reduction.

2. Materials and methods

2.1. Materials

(3S)-Cis-3, 6-Dimethyl-1, 4-dioxane-2, 5-dione (L-lactide), 98%, was purchased from Aldrich chemical company, Inc., USA. Polyethylene glycol 2000 monomethyl ether (MEPEG–PLA), O-(2-Maleimidoethyl)-O′-methyl-polyethylene glycol 5000 (maleimide PEG), ethyl acetate 99.5% ACS reagent, stannous octoate, sulpiride, rhodamine, citric acid, sodium cholate, bovine serum albumin (fraction V) (BSA), ethylene diamine, Snakeskin™ dialysis membrane (MWCO 10,000), SEPHADEX PD 10 column, Traut's reagent (2-Iminothiolane), 5′-dithio-bis (2-nitrobenzoic acid) (DTNB reagent), trichloroacetic acid (TCA), Alexa Fluor® 488 dye, EDAC (*N*-(3-Dimethylaminopropyl)-*N*-ethyl carbodimidehydrochloride), and sodium bicarbonate were purchased from Sigma–Aldrich, USA. Methanol, dichloromethane, ether 98%, toluene 99.8% HPLC grade were purchased from J.T. BAKER, USA. Precast Novex® pH 3–10 IEF gel 1.0 mm, 10-well was purchased from Invitrogen, USA. All the organic solvents used were of analytical grade and were used as received.

2.2. Methods

2.2.1. Polymer synthesis

A ring opening polymerization was employed to synthesize the copolymer of methoxy PEG–PLA (MePEG–PLA) and maleimide PEG–PLA. Briefly, L-lactide 98% was purified twice by recrystallization with dry ethyl acetate. In a schlenk type flask, 2.9225 g L-lactide and 0.229 g maleimide PEG or 0.208 g methoxy PEG were placed. Stannous octoate (20 mg) was added to both polymeric solutions in dried toluene. After 10 vacuum argon cycles, the flask was kept under reduced pressure at 70 °C for 45 min followed by 2 h reaction under argon flow at 110 °C for 2 h. The cooled product was dissolved in dichloromethane (20 mL) and recovered by precipitation in ethyl ether (100 mL). This step was performed twice to ensure the purity of the formulated copolymers [9].

2.2.2. Nanoparticle synthesis

Pegylated NPs were prepared using double emulsion/solvent evaporation method. In a beaker, 0.5 mL of rhodamine (0.2 mg/mL) and 0.5 mL of 1% Na cholate were taken to which organic mixture containing 1.5 mL of sulpiride (2 mg/mL) in dichloromethane and 4-mL mixture of methoxy PEG–PLA (16.66 mg/mL) and maleimide PEG–PLA (8.4 mg/mL) in dichloromethane were added. The solution was homogenized at 38,000 g for 30 s, 10 mL of 1% Na cholate was added and solution was homogenized, diluted further with 0.5% Na cholate. The organic solvent was evaporated using Buchi® rotavaporator for 45 min and centrifuged at 650,000 g using Beckman centrifuge for 45 min and thereafter freeze dried [6,10].

2.2.3. Preparation of cationized bovine serum albumin (CBSA) and BSA-conjugated NPs

BSA (150 mg) was dissolved in 5 mL of 1 M ethylene diamine with deionized distilled water. The pH of amine solution was adjusted to 5 with 1 N hydrochloric acid before dissolving the protein. The reaction was initiated by the addition of 100 mg of EDAC to solution by constant stirring at room temperature. After 5 h, an additional 150 mg of EDAC was added and stirred continuously for another 12 h. The reaction was terminated using 1.3 mL of 4 M acetate buffer, pH 4.75. The solution was then dialyzed overnight using a dialysis membrane (MWCO 10,000) against deionized distilled water with water replacement at least 2–3 times. The solution in the bag was then passed through SEPHADEX® PD 10 column, and purified solution was centrifuged at 1500 g and lyophilized to get ethylene diamine-modified BSA [11]. Cationized and uncationized BSA was dissolved in a non-amine phosphate buffer saline (PBS) pH 8.0, using a 40-fold molar excess of Traut's Reagent. Traut's reagent was dissolved in buffer at a concentration of 2 mg/mL which resulted in a 14 mM stock solution from which 46 μL of solution was pipetted into protein solutions. The solutions were incubated for 1 h at room temperature, and the thiolated protein was separated from excess of Traut's reagent using SEPHADEX® PD 10 column that had been equilibrated with buffer containing 2 mM EDTA [12].

Labeling of protein was performed according to the procedure provided in the fluorescence labeling kit. Solution of sodium bicarbonate (1 M), pH ~ 9.0 was prepared, and 50 μL of the solution was added to 0.5 mL of the 2 mg/mL protein solutions. The protein solutions were transferred to the vial of Alexa Fluor® 488 dye. The reaction mixture was stirred for 1 h at room temperature. The protein solution was passed through a SEPHADEX PD 10 column and thus separated from unconjugated dye [13]. The thiolated CBSA or BSA was mixed with NPs at a thiolated CBSA/BSA: maleimide ratio of 1:1. The volume of mixture was 1 mL, and the conjugation of the CBSA (or BSA) to the NPs loaded with sulpiride was performed overnight on a rotating petri dish at a low speed. The reaction mixture was then applied to SEPHADEX® PD 10 column and was eluted with 0.01 M PBS buffer (pH 7.4). The fluoresced CBSA-NPs fractions or BSA-NPs fractions were identified under UV lamp, collected and freeze dried [14].

As shown in (Fig. 1), the formulation of CBSA-NPs involved several steps including copolymer synthesis to conjugation of fluoresced CBSA protein to the nanoparticles.

2.2.4. Sulpiride assay method development

The stock solution of sulpiride was prepared in methanol, and various dilutions were spiked with fixed amount of rhodamine into plasma. The plasma samples were treated with 30 μL (1 mcg/mL) of tiapiride (internal standard) and 0.1 mL of 1 N NaOH solution. After vortex mixing for 5 s, the mixture was extracted with 6 mL of ethyl acetate: dichloromethane mixture (5:1 v/v), vortexed and centrifuged (168 g) for another 10 min [15]. The supernatant (organic phase) was transferred to another glass tube and evaporated under a stream of nitrogen gas at 40 °C until completely dried followed by the addition of 0.2 mL of the mobile phase to dissolve the residue, and 0.1 mL was automatically injected into the HPLC system for analysis. After plasma extraction, samples were assayed using Nucleodur© column (4.5 mm × 25 cm, 5.0 μm), using a flow rate of 1.2 mL/min with methanol: citrate–phosphate buffer (15:85, pH 3.8) as the mobile phase detected using a fluorescence detector (300 nm excitation, 365 nm emission) and integrated with WATERS EMPOWER©2 software [15]. The results were plotted

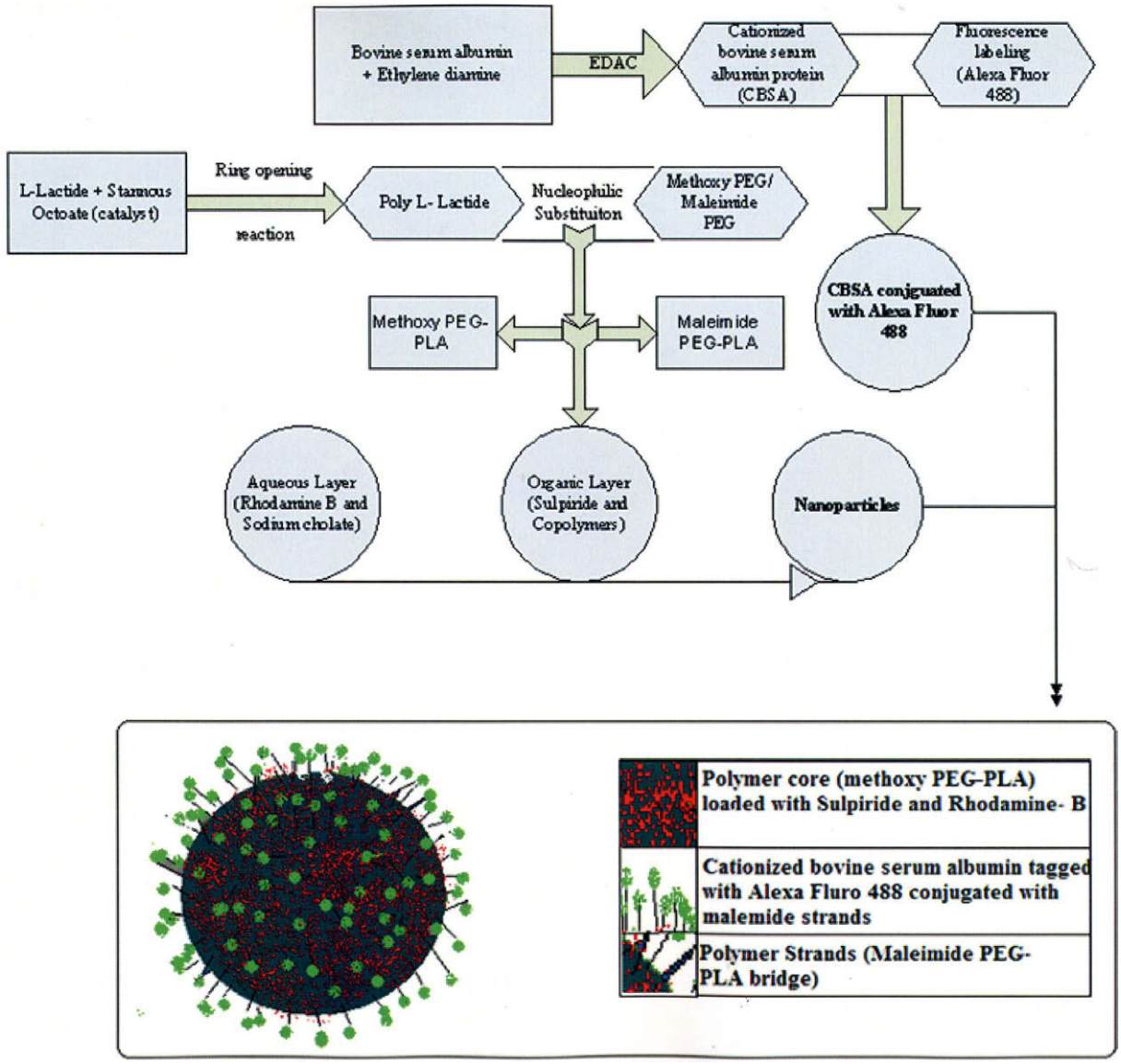

Fig. 1. Schematic of formation of cationized bovine serum albumin-conjugated pegylated nanoparticles. (For interpretation of the references to color in this figure legend, the reader is referred to the web version of this article.)

as ratio of sulpiride response to tiapiride response v/s standard concentration of sulpiride injected.

2.3. Characterization

2.3.1. In vitro studies

2.3.1.1. Copolymer characterization. Both copolymers (MePEG–PLA and MAL PEG–PLA) were dissolved in deuteriochloroform (CDCl3) in NMR analysis tubes. ^{1}H NMR spectra and ^{13}C NMR spectra were recorded at 300 K with a Bruker Avance 500 spectrometer operated at 500 MHZ.

2.3.1.2. Characterization of NPs.

2.3.1.2.1. Surface charge and particle size analysis. The zeta potential and particle size were measured using NICOMP™ 380 ZLS particle size analyzer. NPs/BSA-NPs/CBSA-NPs were suspended in deionized distilled water (1%w/v) in a cuvette, sonicated and measured [14].

2.3.1.2.2. Morphology. Freeze-dried CBSA-NPs, uncoated NPs, copolymers and uncoated drug samples were pre-coated with gold for 120 s using Poloron Sputter coater E-1500 and were observed with the help of Hitachi S-530 scanning electron microscope (SEM) at 25 kV, 6000× [16].

2.3.1.2.3. Cationization of protein. Isoelectric gel electrophoresis was performed using Emperor Penguin P8DS electrophoretic apparatus. During isoelectric focusing (IEF), protein samples were applied to the gel and an electric field was applied, the proteins migrated in the pH gradient and immobilized as they approached their isoelectric point (PI). The Precast IEF gels were loaded with loading sample buffer (10 μL) in one well and mixture of protein standards (10 μL) in second well. The upper electrophoretic chamber was loaded with cathode buffer (200 mL) and lower with anode buffer (600 mL). An increasing order of electric voltage, 100 V (first hour), 200 V (second hour) and finally 500 V (30 min), was applied. High finishing voltage was applied to focus the protein in narrow zones [17].

2.3.1.2.4. Extent of thiolation of protein. Ellman's reagent was used to determine thiol attached to the protein [18]. The dilution buffer (30 mM Tris–HCl, 3 mM EDTA, pH 7.4) and 5,5′-dithio-bis (2-nitrobenzoic acid) (DTNB) solutions were prepared by dissolving 29.7 mg of DTNB in 25 mL methanol. Samples and blank solution (dilution buffer and DTNB reagent) were spined down at 3000 g

for 5 min at room temperature; extinction was measured at 412 nm for total and free thiol groups present. The difference represented the extent of thiolation. Protein was estimated for (i) total sulfhydryl groups (attached to protein and in free form) and (ii) protein precipitated samples using 20% trichloroacetic acid (TCA) (free form) [19].

2.3.1.2.5. Drug load. NPs (10 mg) were dissolved in a mixture of 0.9 mL of dichloromethane and 0.1 mL of dimethylsulphoxide (DMSO). The mixture was evaporated using a rotavaporator at 40 °C until completely dry. The dry samples were reconstituted with the mobile phase, filtered and assayed to determine the drug load by the following equation [1]:

$$\frac{\text{Mass of drug in nanoparticles}}{\text{Total mass of nanoparticles}} \times 100 \quad (1)$$

2.3.2. In vivo studies

CBSA-NPs were explored as targeted drug delivery system to the brain compared to the BSA-NPs and uncoated NPs. Male Sprague Dawley (SD) rats were purchased from Harlan (Indianapolis, IN). Animal study protocol was reviewed and approved by the Saint Johns University Institutional Animal Care and Use Committee. SD rats were divided into three groups; five animals in each group and were restrained using an AIMS restrainer and were administered 10 mg/kg of unconjugated, BSA-conjugated or CBSA-conjugated NPs via lateral tail vein using a 25 g needle and an injection set.

2.3.2.1. Plasma drug release and total urine concentration. Animals were kept in a Beekeeper® cage to collect blood samples (0.5 mL) at 0.5, 1, 2, 4, 8, 16 and 24 h using the tail tip method and analyzed for plasma drug profile of the formulations. Total urine accumulated in 24 h was also collected and analyzed for the presence of sulpiride. After extraction, the samples were diluted with 10 mL of distilled water and were analyzed using the given assay method.

2.3.2.2. Fluorescence microscopic studies. The animals were euthanized using carbon dioxide chamber and organs including brain, liver, spleen and kidney were fixed in 4% formalin solution for 3 days. Later 40-μm thick sections were taken using a microtome, and the sections were directly mounted on slides, frozen and observed under ZEISS® IM fluorescence microscope [20]. The fluorescence images were analyzed for the intensity of color present using Adobe Photoshop software [21]. Briefly, a rectangular area of each image was selected and observed for red or green color intensity as per RGB color intensity model [22]. The average RGB value for each formulation i.e. intensity of fluorescence present was plotted for all formulations using bar plots for brain, kidney, spleen and liver.

2.3.2.3. Statistical analysis. ANOVA was performed to observe statistical differences of sulpiride concentrations for CBSA, BSA and uncoated NPs formulation in terms of plasma profile and total urine excretion. Student *t*-test and ANOVA were performed to show significant difference of fluorescence intensity in microscopic sections of brain for CBSA, BSA and uncoated NP's formulations.

3. Results and discussion

3.1. Copolymer synthesis

The ^{1}H NMR data (Fig. 2) showed both polymers were present in the final formulation [23]. The peaks at 1.65 ppm belonged to methyl group (–CH3) and 5.20 ppm pertained to methine group (–CH–) of PLA segment. The methene group (–CH2–) of PEG segment appeared at 3.65 ppm. A low-signal peak integral at 6.65 ppm corresponding to the maleimide protons was detected that proved the preservation of the maleimide function during the synthesis of maleimide PEG–PLA [24], no other peaks were detected, which indicated high purity of the copolymers. The ^{13}C NMR data (Fig. 2) shows a change in C═O chemical shift from 168 ppm to 169 ppm attributed to the broken cyclic ring of L-lactide with nucleophilic substitution.

3.2. Change in isoelectric focal point (IEF)

IEF is an electrophoretic technique for the separation of proteins based on their isoelectric point (pI), the pH at which a protein has no net charge and does not migrate in an electric field. These are used to determine minor changes in the nature of protein such as cationization, phosphorylation and glycosylation. The pI of native albumin is relatively low i.e. 4 (acidic) due to the presence of carboxyl group on surface of protein. Substitution of basic groups in place of carboxyl groups can increase the pI of protein towards more basic pI i.e. 8–11. Cationization of the BSA changed pI from 4.2 to 8.3 (Fig. 3) which had an impact on overall formulation as the surface charge distribution (zeta potential) of formulation changed for CBSA-NPs with respect to BSA/uncoated NPs as highly basic proteins (pI: 8–11) can adsorb to the endothelial cells of the blood–brain barrier at higher rates than that for acidic and neutral proteins [25].

3.3. Extent of thiolation

Ellman's reagent undergoes the thiol-disulphide interchange reaction in the presence of a free thiol. The resultant 2-Nitro-5-Mercapto benzoic acid formed had an intense absorbance at 412 nm compared to reagents [26]. At high or low pH the disulphide splits and hence the reaction was performed at neutral pH with an excess of DTNB to protein. The concentration was calculated using Eq. (2) (where, A = absorbance of solution, b = path length in cm^{-1}, and ε = molar absorptivity in $L\,cm^{-1}\,mol^{-1}$). The extent of thiolation was 86 ± 10%.

$$\text{Concentration} = \frac{A}{b * \varepsilon} \quad (2)$$

3.4. Surface charge changes and average particle size

The zeta potential (ζ value) represents the difference in the electrical charge between the dense layers of ions that surrounds the particle and the charge of the bulk of the suspended fluid surrounding the particles. The ζ value of CBSA-NPs could be attributed to two factors, first the PEG surface shielding effect on offsetting the negative charge of the PLA segments in the NPs core and second, the CBSA cationization degree i.e. pI value. The ζ values measured for uncoated NPs and CBSA-NPs were around −39 mV and −19 mV, respectively. The potential difference in ζ values represents successful attachment of CBSA to NPs and change in surface charge property of the particle. Although ζ value for the obtained particle was towards negative side, it supported our hypothesis; because at the local microenvironment surrounding each CBSA milieu on the NPs surface, the net electrical charge would be positive. Hence, facilitating CBSA at periphery of the NPs to electrostatically bind the negatively charged residues on the endothelial cells of BBB. Therefore it could be assumed that due to relatively less negative surface charge of the particle, it gets attracted and adsorbed to the BBB endothelial cells and thus enhances the availability. The average particle size of plain NPs was 218 ± 10 nm, BSA-NPs was 308 ± 24 nm and CBSA-NPs was 329 ± 44 nm. Once sufficiently reduced, the particle gets internalized to reach to the site of action. Thus, the drug could reach the site of action in free

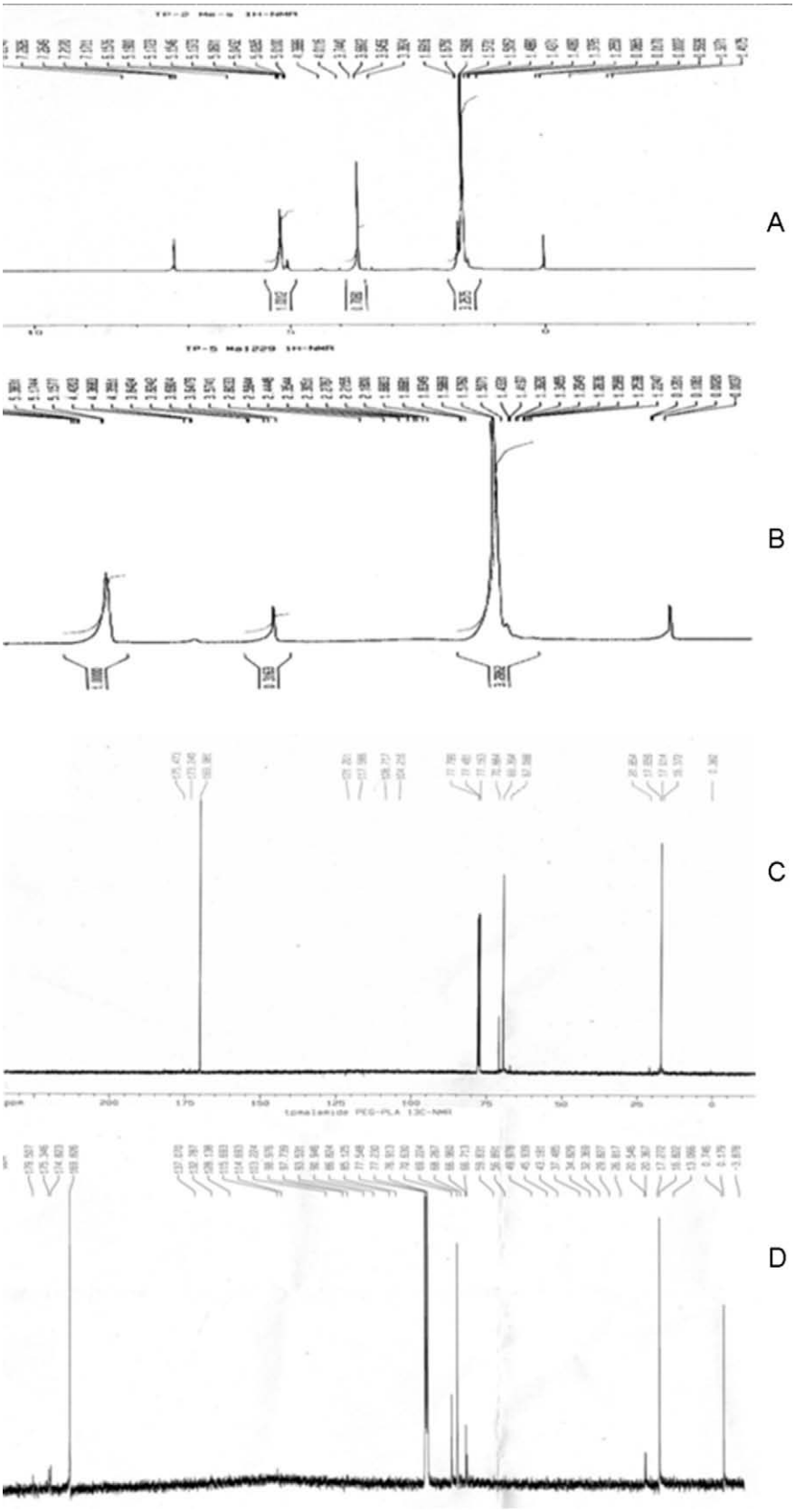

Fig. 2. ^{1}H NMR Data: (A) methoxy PEG–PLA and (B) maleimide PEG–PLA. Peaks: PLA segment (a) 1.65 ppm-methyl group (–CH3) and (b) 5.20 ppm-methine group (–CH); PEG segment (a) 3.65 ppm-methene group. ^{13}C NMR Data: (C) methoxy PEG–PLA and (D) maleimide PEG–PLA C═O chemical shift at 169 ppm due to breakage of cyclic lactide ring.

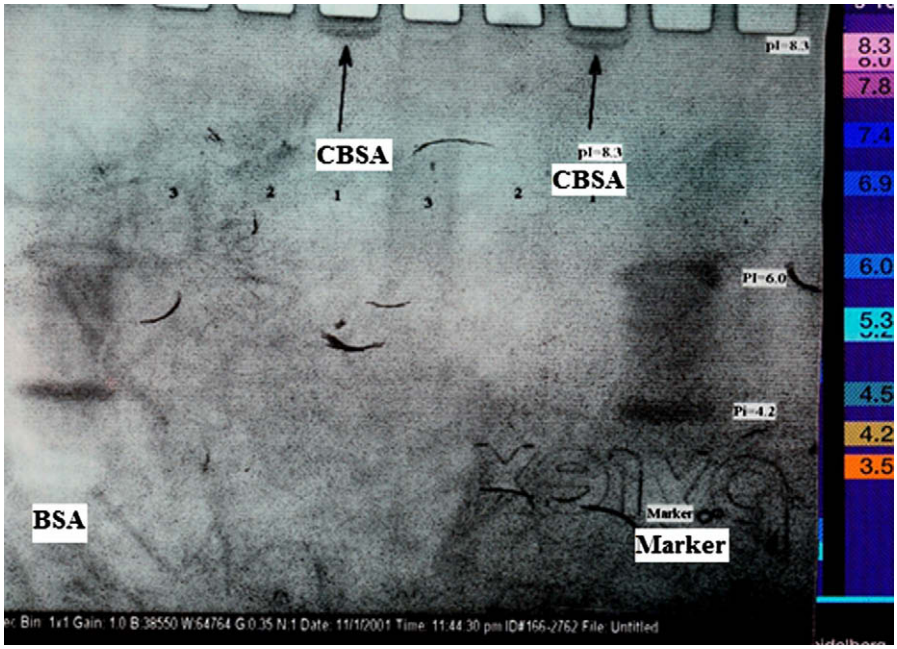

Fig. 3. Isoelectric focusing: right band indicates different pH range in the gel. CBSA protein pI: 8.3 (third well and sixth well from right side). BSA protein pI: 4.2. Comparative standard band (second from right side) shows separation of different proteins based on pI. (For interpretation of the references to color in this figure legend, the reader is referred to the web version of this article.)

form and in NPs bound form. This approach had two advantages, improved drug loading due to larger size of NPs when compared to others for brain delivery as well as target delivery of the drug at the site of action [27].

3.5. Morphological observations

The scanning electron microscopy showed that copolymers were rough, irregular and hollow structures. The final formulation on the other end was spherical in shape (Fig. 4) because of the surface tension on emulsion droplets causing the copolymers to form spherical shape and entrapping the drug in its matrix during solvent evaporation.

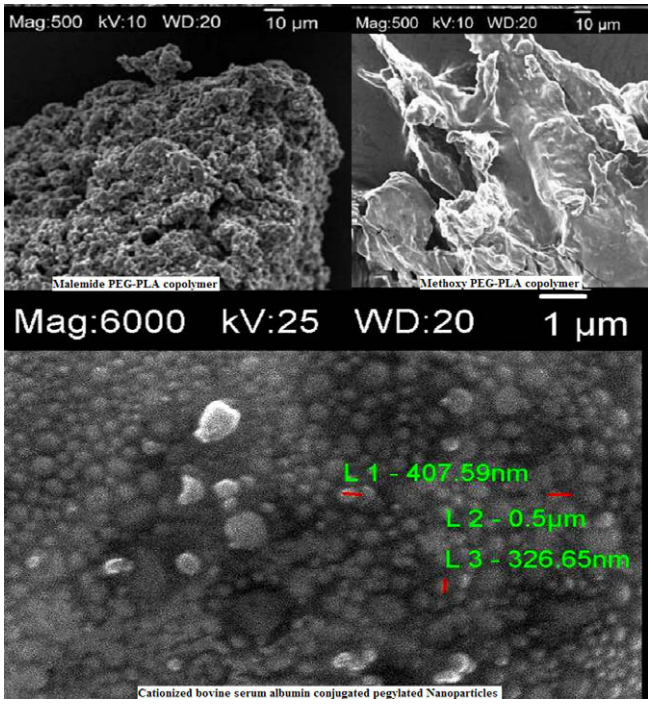

Fig. 4. Scanning electron microscopy. (1) Maleimide PEG–PLA copolymer. (2) Methoxy PEG-\PLA copolymer. (3) Cationized bovine serum albumin-conjugated nanoparticles. (For interpretation of the references to color in this figure legend, the reader is referred to the web version of this article.)

3.6. Standard curve and drug loading efficiency (DLE)

To extract sulpiride from plasma, a mixture of ethyl acetate and dichloromethane was used. Dichloromethane (BP 39 °C) and ethyl acetate (BP 77 °C) gave an effective separation when used in combination rather than separate as sulpiride was more soluble in ethyl acetate while dichloromethane with low boiling point was easy to evaporate [28]. The extent of sulpiride extraction from plasma was 62.25 ± 4.03%. A Sigma plot for ratio of sulpiride to tiapiride response was plotted with respect to standard sulpiride concentrations. The assay was validated with respect to linearity (R^2 = 0.9933), limit of detection (0.05 µg/ml) and limit of quantitation (0.1 µg/ml). The drug loading (DLE) of NPs was 4.34 ± 0.88%, n = 3.

3.7. In vivo plasma and urine study

The blood samples were extracted and detected using HPLC fluorescence assay method. The in vitro release of plain NPs (30% release in 10 h) [29] and the fact that NPs were incubated with albumin solution for 10 h to conjugate with NPs suggested the necessity to normalize the results obtained due to reduced sulpiride and rhodamine B load of CBSA-NPs/BSA-NPs when compared to plain NPs. Thus, the final plot was obtained after this normalization of data. Sulpiride concentration detected was plotted as log plasma concentration of sulpiride (µg/ml) vs. time (h) (Fig. 5) with large amount of drug released in first 5 h after which low concentration of drug was detected for CBSA-NPs when compared to other two formulations. (Fig. 5) The decrease in the release of sulpiride in plasma for CBSA-NPs could be possible if the formulation was behaving differently, suggesting that either it was cleared out faster through urine or it was biodistributed at a faster rate. The cumulative average percentage of urinary excretion for albumin-

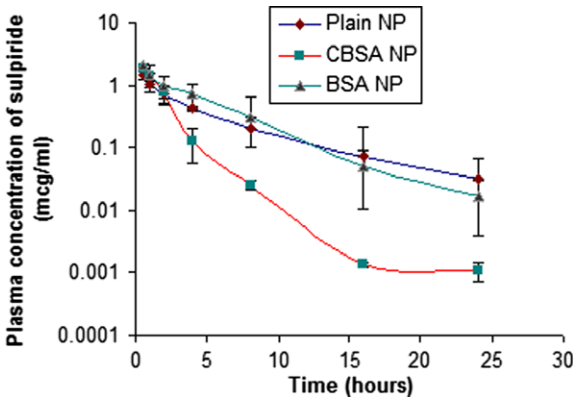

Fig. 5. Sulpiride plasma concentrations (mcg/ml) of Sprague Dawley rats ($n = 5$) for (1) plain nanoparticles (—◆—), (2) BSA nanoparticles (—■—), and (3) CBSA nanoparticles (—▲—) vs. time (h), respectively. A lower percentage plasma dose release profile for CBSA nanoparticle (60.42 ± 8.57%) obtained when compared to BSA nanoparticles (86.23 ± 18.32%) and uncoated nanoparticles (82.35 ± 12.25%). (For interpretation of the references to color in this figure legend, the reader is referred to the web version of this article.)

conjugated and unconjugated NPs was 19.26 ± 0.66% after 24 h, very low when compared to 70–90% of sulpiride excretion as mentioned in literature [7,8]. Thus, NPs had tremendously reduced the excretion of sulpiride in urine. Statistically, there was no significant variation in percentage of drug urine excretion from animals with different formulations ($p < 0.0773$), which excludes the possibility of higher urinary excretion of CBSA-NPs when compared to BSA/uncoated NPs and strengthens the possibility of particles sustained and biodistributed in the body.

3.8. Fluorescence microscopy studies

A qualitative distribution of CBSA-NPs compared to BSA/uncoated NPs was observed via fluorescence distribution in microscopic sections helped to pre-screen the formulations (Fig. 6). However, quantification of these images viz. a procedure answering; degree of variance of fluorescence in different organs for different formulations could provide a better tool for comparison. For this, spectroscopic methods have been used extensively for quantitation but in our case the amount of rhodamine B [30] and Alexa Fluor® 488 [13] used in NPs was very low which increases the error in measurement at such low concentrations. Once the variability of repeated measurements within and between samples was acceptable, we selected the Adobe Photoshop® software tool to calculate the intensity of the color present in the images because a single color (green or red) was present in each image (depending upon the filters used while taking images) (Fig. 6). The images varied upon intensity of the fluorescence (the amount of rhodamine B or Alexa Fluor 488) and hence upon the amount of distribution of particles in that organ. Thus, it proved to be a time efficient, easier and cheaper tool to pre-screen the target efficiency of the formulation and to understand the distribution of the particles in major organs depending upon the formulation administered.

Adobe Photoshop® software provided an average numerical value (RGB value) for the intensity of color present in an image as per RGB model; by comparing the values obtained in all formulations following results were inferred. As observed in (Fig. 7), the fluorescence intensity of CBSA-NPs sections in brain was very high when compared to the BSA-NPs and uncoated NPs ($p = 0.000874$) which could be a result of higher adsorption of CBSA-NPs to the brain endothelial cells when compared to other two formulations. A high level of fluorescence intensity was observed in the liver and spleen sections (Fig. 7) in all the formulations suggesting that NPs generally had a high distribution in these organs. In liver, the major reason for distribution could be the filtration barrier formed by splenic and hepatic cord and in spleen due to the phagocytes present in the Kupffer cells in spleen which engulfs and remove the nanoparticles from systemic circulation. In case of kidney (Fig. 7) CBSA-NPs had least distribution compared to uncoated/BSA-NPs again supporting our hypothesis as cationization minimizes renal clearance. A student *t*-test was performed to analyze the variance between the RGB values in brain of BSA-NPs and CBSA-NPs ($p < 0.01530$) proved that they were significantly different; and thus the high uptake in brain was not due to the presence of albumin protein but due to the positive charge on the protein. Literature shows that a majority of endothelial cells of the blood–brain barrier are negatively charged due to sialic acid residues of acidic glycoprotein mainly concentrated in the cells of central nervous system; [31,32].The positive charge of the CBSA-NPs compared to plasma proteins facilitated an attractive force and increased contact to such regions. Once adsorbed, NPs started degrading and smaller size NPs formed were taken up via BBB possibly by adsorptive-mediated transcytosis [31].

In summary, the accumulation of rhodamine B was non-specific to brain tissue, proved from liver and spleen color intensity

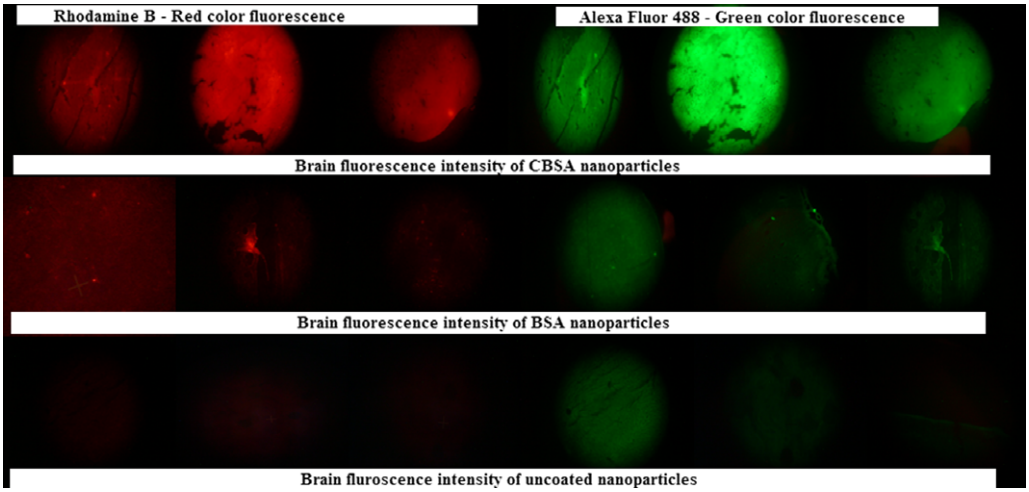

Fig. 6. Brain fluorescence microscopy sections (from top to bottom). (1) CBSA nanoparticles, (2) BSA nanoparticles, and (3) uncoated nanoparticles. Order of fluorescence emitted was highest for CBSA-NPs sections followed by BSA-NPs and least in uncoated NPs sections (red – rhodamine B fluorescence, green – Alexa Fluor 488 fluorescence). (For interpretation of the references to color in this figure legend, the reader is referred to the web version of this article.)

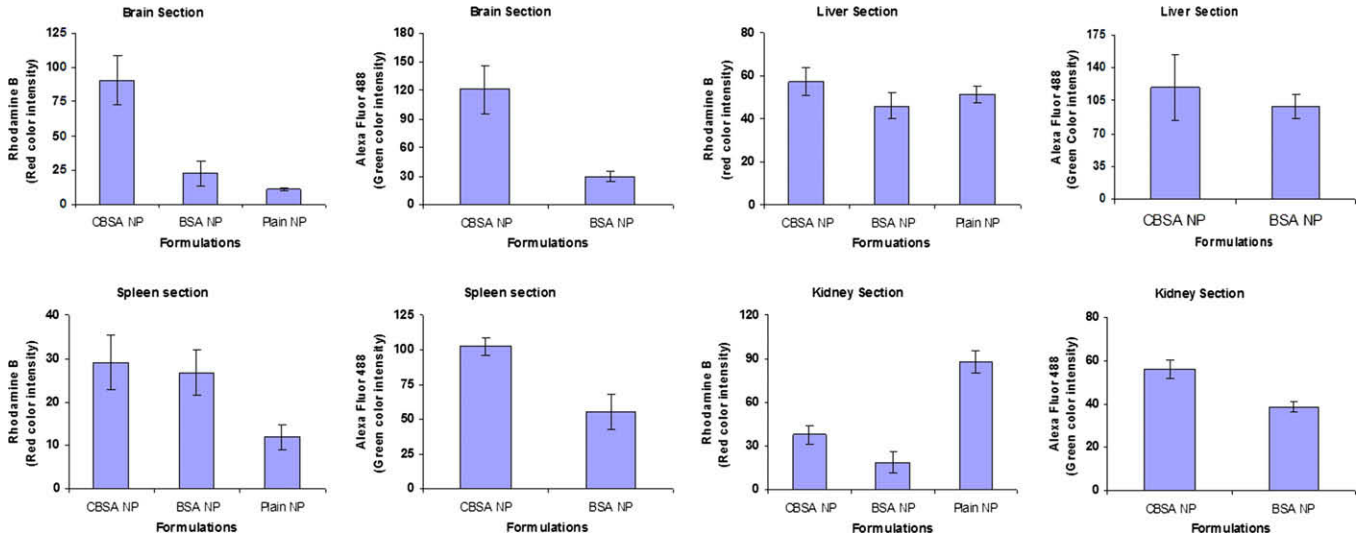

Fig. 7. Comparison of color intensity measured by Adobe Photoshop software (from top-left to bottom-right) (1) CBSA-NPs, (2) BSA-NPs, and (3) uncoated NPs in brain, liver, spleen and kidney sections for fluorescence emitted by rhodamine B and Alexa Fluor 488 dye. (For interpretation of the references to color in this figure legend, the reader is referred to the web version of this article.)

measurements. A high distribution of CBSA-NPs was observed in liver and spleen sections but it was in accordance with that of uncoated and BSA-NPs, indicating that the positive charge was not a major factor for accumulation in these organs. On the other end, variance observed in brain sections established that the surface charge of NPs was the driving factor for delivery to brain and provided us with a novel method to pre-screen formulations. These results are significant as they logically proceed to a promise afforded by the reduction in the dose of marketed oral formulations (e.g., Dogmatil Forte®) alluded in the Introduction section. In the form of CBSA-NPs we formulated a considerable delivery system that could provide a single solution to the problems associated with delivery of sulpiride, reduced excretion in urine hence improved bioretention, targeting the drug to site, and thus reduction in dose of the drug.

4. Conclusion

Polymeric NPs conjugated with CBSA or BSA were successfully formulated. All the results and statistical evaluation can be combined to conclude that CBSA-NPs has faster clearance from the plasma relative to either BSA-NPs or uncoated NPs and that this clearance was not so much elimination but rather a targeted distribution by preferential uptake into the brain. Urinary observations and fluorescent images showed that CBSA-NPs had high biodistribution in several organs, most notably the brain, compared to BSA-NPs and uncoated NPs. This localization in the target tissue by fluorescent imaging was an efficient analytical pre-screening tool for accelerating the dosage form development process of NPs that incorporate sulpiride. These results confirm our hypothesis that a PEG–PLA copolymer-based nanoparticulate system when conjugated with CBSA can provide a targeted drug delivery of sulpiride.

References

[1] M. Smith, M. Gumbleton, Endocytosis at the blood–brain barrier: from basic understanding to drug delivery strategies, J. Drug. Target. 14 (2006) 191–214.
[2] W. Lu, Y. Zhang, Y. Tan, K. Hu, X. Jiang, S. Fu, Cationic albumin-conjugated pegylated nanoparticles as novel drug carrier for brain delivery, J. Control Release 107 (2005) 428–448.
[3] J. Kreuter, Colloidal Drug Delivery Systems, first ed., Marcel Dekker, Inc., 1994.
[4] S. Stolnik, L. Illum, S. Davis, Long-circulating microparticulate drug carriers, Adv. Drug. Deliver Rev. 16 (1995) 195–214.
[5] W. Lu, J. Wan, Z. She, X. Jiang, Brain delivery property and accelerated blood clearance of cationic albumin conjugated pegylated NPs, J. Control Release 118 (2007) 38–53.
[6] W. Lu, Y. Tan, X. Jiang, Cationic albumin conjugated pegylated NPs with its transcytosis ability and little toxicity against blood–brain barrier, Int. J. Pharm. 295 (2005) 247–260.
[7] N. Muller, R. Dessing, European Drug Index, fourth ed., CRC Press, 1997.
[8] F. Wiesel, G. Alfredsson, M. Ehrnebo, G. Sedvall, The pharmacokinetics of Intravenous and oral sulpiride in healthy human subjects, Euro. J. Clin. Pharmaco. 17 (1995) 385–391.
[9] J. Olivier, R. Huertas, F. Calon, W. Pardridge, Synthesis of pegylated immunonanoparticles, Pharm. Res. 19 (2002) 1137–1143.
[10] K. Wadhwani, S. Rapoport, Enhanced permeabilities of cationized-bovine serum albumins at the blood–nerve and blood–brain barriers in awake rats, J. Neurosci. Res. 32 (2004) 407–414.
[11] J. Futami, T. Maeda, M. Kitazoe, T. Nukui, M. Seno, Preparation of potent cytotoxic ribonuclease by cationization: enhanced cellular uptake and decreased interaction with ribonuclease inhibitor by chemical modification of carboxyl groups, Biochemistry (2001) 7518–7524.
[12] A. Tarentino, 2-Iminothiolane: a reagent for the introduction of sulfhydryl groups into oligosaccharides derived from asparagine-linked glycans, Glycobiology 3 (1993) 279–285.
[13] K. Triantafilou, M. Triantafilou, N. Fernandez, Lipopolysaccharide (LPS) labeled with Alexa 488 hydrazide as a novel probe for LPS binding studies, Cytometry 41 (2000) 316–320.
[14] D. Hoare, Koshland Jr., A method for the quantitative modification and estimation of carboxylic acid groups in proteins, J. Biol. Chem. 242 (1967) 2447–2453.
[15] S. Jin, E. Ban, Y. Kim, C. Kim, Development of HPLC method for the determination of levosulpiride in human plasma, J. Pharm. Biomed. Anal. 35 (2004) 929–936.
[16] S. Hatziantoniou, Y. Nikas, G. Deli, Scanning electron microscopy study on nanoemulsions and solid lipid nanoparticles containing high amounts of ceramides, Micron 38 (2007) 819–823.
[17] W. Pardridge, P. Schimmel, Cationized Antibodies for Delivery through the Blood–Brain Barrier, US Patent 5004697, 1989.
[18] G. Bulaj, T. Kortemme, D. Goldenberg, Quantitation of sulfhydryl DTNB, Ellman's reagent, Biochemistry 37 (1998) 8965–8972.
[19] S. Gill, P. Hippel, Calculation of protein extinction coefficients from amino acid sequence data, Anal. Biochem. 182 (1989) 319–326.
[20] S. Rogers, Biological Application of Fluorescence Microscopy, Technical Report 99-006, 1999, pp. 3–18.
[21] J. Chawla, M. Amiji, Biodegradable poly(ε-Caprolactone) nanoparticles for targeted delivery of tamoxifen, Int. J. Pharm. 249 (2002) 127–138.
[22] M. Evening, Color Management, Adobe Photoshop CS for Photographers, 2004, pp. 354–407.
[23] Y. Dong, S. Feng, Methoxy poly(ethylene glycol)–poly(lactide) nanoparticles for controlled delivery of anticancer drugs, Biomaterials 25 (2004) 2843–2849.
[24] Y. Zhang, L. Zha, C. Wang, S. Jiang, Preparation characterization and application of pyrene-loaded methoxy poly(ethylene glycol)–poly(lactic acid) copolymer nanoparticles, Colloid Polym. Sci. 282 (2004) 1323–1328.
[25] G. Friedli, Interaction of Deamidated Soluble Wheat Protein with Other Food Proteins and Metals. Unpublished Results, 1996.
[26] J. Dean, Lange's Handbook of Chemistry, 14th ed., Mc Graw-Hill, 1999.

[27] T. Govender, S. Stolnik, L. Illum, PLGA Nanoparticles prepared by nanoprecipitation: drug loading and release studies of a water soluble drug, J. Control Release 57 (1999) 171–185.
[28] J. Liu, W. Cao, X. Sun, Determination of sulpiride by capillary electrophoresis with end-Column electro generated chemiluminescence detection, Clin. Chem. 48 (2002) 1049–1058.
[29] N. Bhatt, R. Gheewala, Optimization of Physicochemical Factors Affecting Drug Loading of Sulpiride Loaded Nanoparticles, Unpublished Results, Saint Johns University, NY, 2008.
[30] R. Guss, F. Johnson, D. Maurice, Rhodamine B as a test molecule in intraocular Dynamics, Invest. Ophthalmol. 25 (1984) 758–762.
[31] R. Horton, L. Moran, R. Ochs, J. Rawn, K. Scrimgeour, Lipids and Membranes, third ed., Prentice Hall, 2002 (Prin. Biochem).
[32] Y. Jallouli, A. Paillard, J. Chang, E. Sevin, D. Betbeder, Influence of surface charge and inner composition of porous nanoparticles to cross blood–brain barrier *in vitro*, Int. J. Pharm. 344 (2007) 103–109.